GEOLOGIA • 2010 • Tom 36 • Zeszyt 2 • 187–202

# VISUALIZATION OF MAGNETOTELLURIC DATA WITH APPARENT VELOCITY METHOD

## Wizualizacja danych magnetotellurycznych przy zastosowaniu metody prędkości pozornej

**Juliusz MIECZNIK & Wojciech KLITYŃSKI**

*Akademia Górniczo-Hutnicza, Wydział Geologii, Geofizyki i Ochrony Środowiska;*
*al. Mickiewicza 30, 30-059 Kraków;*
*e-mail: j_miecznik@poczta.onet.pl, gpklityn@geolog.geol.agh.edu.pl*

**Abstract:** Magnetotelluric (MT) field data are usually presented as plots of amplitude and phase MT sounding data vs frequency. Visualization of resistivity changes of geoelectric complexes with the use of apparent resistivity and phase curves give qualitative results only. Quantitative interpretation of MT sounding curves is needed to get geoelectric parameters. For a 1D horizontally layered earth, amplitude curves (apparent resistivity curves) and phase curves can be transformed into apparent velocity curves versus depth of EM field penetration into the conducting earth.Apparent velocity curves can be approximated by straight-line segments corresponding to homogeneous geoelectric layer complexes. Each segment of the apparent velocity curve (with a given angle of inclination) is related with the resistivity and thickness of individual geoelectric complexes. For heterogeneous earth (2D or 3D) vertical component of the magnetic field is directly connected with boundary of geoelectric complexes. It can be used to express components of vectors of apparent velocity. For a 1D horizontally layered earth, a vector of apparent velocity has only the vertical component. For heterogeneous earth horizontal components of apparent velocity also are inducted. The angle of inclination of the total vector of velocity and its value depend on the geometry of studied structure.

**Key words:** magnetotelluric sounding, visualization, apparent velocity, depth of penetration

**Treść:** Podstawową wielkością prezentującą zmiany przewodnictwa elektrycznego górotworu z głębokością jest oporność pozorna jako funkcja częstotliwości pola magnetotellurycznego. Wizualizacja tych zmian, jak również granic struktur geologicznych, przez oporność pozorną ma charakter jedynie jakościowy, dalece przybliżony. Parametry przekroju geoelektrycznego uzyskujemy jedynie przez interpretację ilościową danych pomiarowych. W przypadku przekrojów geoelektrycznych 1D krzywe sondowań magnetotellurycznych możemy przetransformować w krzywe prędkości pozornej jako funkcje głębokości wnikania pola elektromagnetycznego w głąb badanego ośrodka. Krzywe te możemy aproksymować odcinkami linii prostych, a kąty nachylenia poszczególnych odcinków względem osi głębokości i ich punkty przecięcia są ściśle związane z opornościami i miąższościami poszczególnych warstw geoelektrycznych. W przypadku ośrodków niejednorodnych 2D i 3D wielkością bezpośrednio związaną z granicami kompleksów geoelektrycznych jest pionowa składowa pola magnetycznego. Przez tę wielkość możemy wyrazić składowe wektora prędkości pozornej. W obszarach 1D wektor prędkości redukuje się do składowej pionowej, natomiast w obszarach niejednorodnych generują się również składowe poziome. Kąt nachylenia całkowitego wektora prędkości do poziomu i jego długość są ściśle związane z geometrią badanej struktury.

**Słowa kluczowe:** sondowanie magnetotelluryczne, wizualizacja, prędkość pozorna, głębokość penetracji

## INTRODUCTION

Magnetotelluric field data are usually presented as plots of amplitude and phase of MT sounding data vs frequency. For a 1D horizontally layered earth, amplitude curves (apparent resistivity curves) reflect resistivity sequence for layers provided that the layers thickness ratio is sufficiently big. For heterogeneous earth (2D or 3D), the shape of the sounding curves depends not only on electric conductivity distribution alone but also on the azimuth of the measurement array axis. This can result in the ambiguous outcome of MT data interpretation. The response of a 2D medium is different for electric polarization and magnetic polarization.

Few attempts at presenting MT data in a different form than the amplitude and the phase of MT field vs frequency can be found in the geophysical literature. Molochnov (1968) proposed the transformation of amplitude MT curves into curves of effective (apparent) depth of electromagnetic field penetration into a conducting earth. As compared to standard methods, the smaller frequency range is sufficient to quantitative interpretation of MT sounding curves transformed in such a way. It is advantageous because of the noise present in the magnetotelluric measurement data. Lack of phase curves causes that the interpretation of magnetotelluric data is less effective.

Taking advantage of the fact that electromagnetic energy is reflected from the boundaries of geoelectric earths and passes through them, the pseudo-impulse response of the earth can be created based on measured amplitudes and phases of EM field (Levv *et al*. 1988).

A time section is composed of discrete impulses whose amplitude depends on reflection coefficient and transition coefficient at geoelectric boundaries. The time of a pulse traveling to the ground surface is twice as big as the time of pulse traveling from the ground surface to the reflecting boundary. An impulse sections constructed along the magnetotelluric profile has a form similar to the time section in the reflection seismic.

Generally, the electromagnetic field used in magnetotellurics satisfies the diffusion equation. If we put $\sqrt{t}$ instead of $t$, then the diffusion equation is transformed into the classic wave equation. As in the former case, the time section in the $\sqrt{t}$ domain is similar to the time section in the reflection seismics (Lee *et al*. 1989, Lee & Xie 1993).

## PRINCIPLES OF APPARENT VELOCITY METHOD

The conservation law of electromagnetic (EM) energy (Wainstain 1963)

$$\frac{\partial \overline{w}}{\partial t} + \overline{p} + \frac{\partial \overline{S}}{\partial r} = 0 \tag{1}$$

where:

$\overline{w}$ – average density of EM energy,
$\overline{p}$ – average density of EM loss,
$\overline{S}$ – average of total Poyting vector (absolute value of electric and magnetic fields),
$r$ – direction of propagation of EM energy.

The averaging is done over the EM field variation period, so for monochromatic wave

$$\frac{\partial \overline{w}}{\partial t} = \text{const} \tag{2}$$

Let us consider a signal of an arbitrary shape. Time $t_o$ to of arrival of the centre of the signal to the observation site is given. The velocity of propagation of the signal is defined as

$$V = \frac{dz}{dt_0} \tag{3}$$

where $z$ – distance.

For a 1D non-attenuating medium we may assume $\overline{p} = 0$ and therefore for quasi--monochromatic signals we get

$$\frac{dz}{dt_0} = V_g = \frac{\overline{S}_z}{\overline{w}} \tag{4}$$

where $V_g$ is the group velocity of the signal and $\overline{S}_z$ is the vertical component of the Poyting vector.

In the case of an attenuating medium and quasi-monochromatic signals expression (4) takes the form

$$V = \frac{V_g}{1 + \alpha(t_0 - t_1)} \tag{5}$$

where $\alpha = \frac{\overline{p}}{\overline{w}}$ and $t_1 = \frac{\int t \cdot \overline{p} dt}{\int \overline{p} dt}$ (Miecznik & Czerwiński 2001).

It is easy to prove that for an attenuating medium and parameters of this medium with which are deal in practice we have the relation

$$\alpha(t_0 - t_1) << 1 \tag{6}$$

The difference $(t_0 - t_1)$ may be interpreted as a delay impulse of loss in relation to impulse of electromagnetic energy. Putting relation (6) into relation (5) we get for velocity of quasi-monochromatic impulses

$$V \approx V_g = \frac{\overline{S}_z}{\overline{w}} \tag{7}$$

For a non-homogeneous (2D, 3D) and attenuating medium the velocity of electromagnetic signals may be described by relation

$$V = \frac{\overline{S}_z}{\overline{w}} \tag{8}$$

where $\overline{S}$ is the mean value of the Poyting total vector, is the mean density of EM energy.

Taking advantage of the theorem on products and squares of complex amplitudes and assuming that the ratio of the impedance of a conducting medium and the impedance of the vacuum is much less than one we can write for the Cartesian coordinates of velocity of electromagnetic field propagation and non-homogeneous medium:

$$V_x = \frac{2}{\mu} \cdot \frac{E_y \cdot H_z}{H^2} \cdot \cos \varphi_{yz} \tag{9a}$$

$$V_y = \frac{2}{\mu} \cdot \frac{E_x \cdot H_z}{H^2} \cdot \cos \varphi_{xz} \tag{9b}$$

$$V_z = \frac{2}{\mu} \cdot \frac{E_x \cdot H_y \cdot \cos \varphi_{xy} + E_y \cdot H_x \cdot \cos \varphi_{yx}}{H_n^2} \tag{9c}$$

where:

$E_x, E_y, H_x, H_y, H_z$ – Cartesian components of electric and magnetic field,

$H^2 = H_x^2 + H_y + H_z^2$ – total vector of magnetic field to the power of two,

$H_n^2 = H_x^2 + H_y^2$ – horizontal vector of magnetic field to the power of two,

$\varphi_{xy} = \varphi_{Ex} - \varphi_{Hy}$,

$\varphi_{yx} = \varphi_{Ey} - \varphi_{Hx} + \pi$,

$\varphi_{xz} = \varphi_{Ex} - \varphi_{Hz}$,

$\varphi_{yz} = \varphi_{Ey} - \varphi_{Hz}$,

$\mu = 4\pi \cdot 10^{-7}$ H/m.

The total velocity vector is expressed by the Cartesian components

$$V = (V_x^2 + V_y^2 + V_z^2)^{1/2} \tag{10}$$

It can be easily proven that relation (10) is the invariant of azimuth of horizontal axes of the Cartesian co-ordinate system.

Expressions (9) and (10) may be described by components of the impedance tensor

$$Z = \begin{bmatrix} Z_{xx} & Z_{xy} \\ Z_{yx} & Z_{yy} \end{bmatrix} \tag{11}$$

Expressions (9) allow two amplitude curves and two phase curves (TM mode and TE mode respectively), which we measured in one measurement site, to be transformed into one curve of apparent velocity versus depth to which EM field propagates into conducting non-homogeneous medium.

2D and 3D geoelectrical models generate the vertical components of magnetic field.

In our geoelectric models the differentiation of electric resistivity at the vertical boundaries is very small therefore the vertical component of magnetic field may be neglected.

Then, the velocity vector has only the vertical component, which has the form

$$V_a = \frac{2}{\mu}\left( \frac{Z_{xy} \cdot \cos\varphi_{xy}}{1+ h_{xy}^2} + \frac{Z_{yx} \cdot \cos\varphi_{yx}}{1+ h_{yx}^2} \right) \tag{12}$$

where $Z_{xy}$ and $Z_{yx}$ are components of the impedance tensor, $\varphi_{xy}$ and $\varphi_{yx}$ are phase shifts of components of magnetic field and electric field, $h_{xy} = \left| \frac{H_x(\omega)}{H_y(\omega)} \right|$, $h_{xy} = h_{xy}^{-1}$, $\omega = 2\pi f$, and $f$ is frequency of MT field variations. It is accepted in the presented calculations that $h_{xy} = h_{yx} = 1$.

Apparent velocity curves are plotted versus EM field penetration depth

$$\delta = \frac{1}{2\pi} \cdot \sqrt{10^{-7} \cdot \frac{\rho_m}{f}} \tag{13}$$

where $\rho_m = \sqrt{\rho_{a_E} \cdot \rho_{a_H}}$ and $\rho_{a_E}$ (TE mode) $\rho_{a_H}$ and (TM mode) are apparent resistivities for the electric polarization and magnetic polarization, respectively, calculated for given frequency (Miecznik *et al*. 2002).

Based on formulas (12) and (13) apparent resistivity and phase curve can be transformed to the apparent velocity curve $V_a$ versus depth of penetration into conductive mediumd, i.e. $V_a = f(\delta)$.

## BASIS OF VISUALIZATION OF MAGNETOTELLURIC SOUNDING

A curve of apparent velocity $V_a$ versus depth of EM field penetration into the conducting earth ($\delta$) can be approximated by straight-line segments corresponding to homogeneous geoelectric layer complexes. First derivative of $V_a(\delta)$ for this segment is constant (second derivative equals zero, in theory, and has relatively low value in practice). On the geoelectric boundaries (inclination of $V_a(\delta)$ changing angle) first derivative changes its value (second derivative of $V_a(\delta)$ has relatively big value). Each segment of the apparent velocity curve can be approximated by function

$$V_a = C \cdot \delta^{-n} \tag{14}$$

where $C$ and $n$ are constants. Constant $n$, which is the tangent of an angle of inclination of individual $V_a$ segment to the depth axis, is related with the resistivities of individual geoelectric complexes.

An example of such transformation for 2D synthetic models is shown in figures 1 and 2.

A)

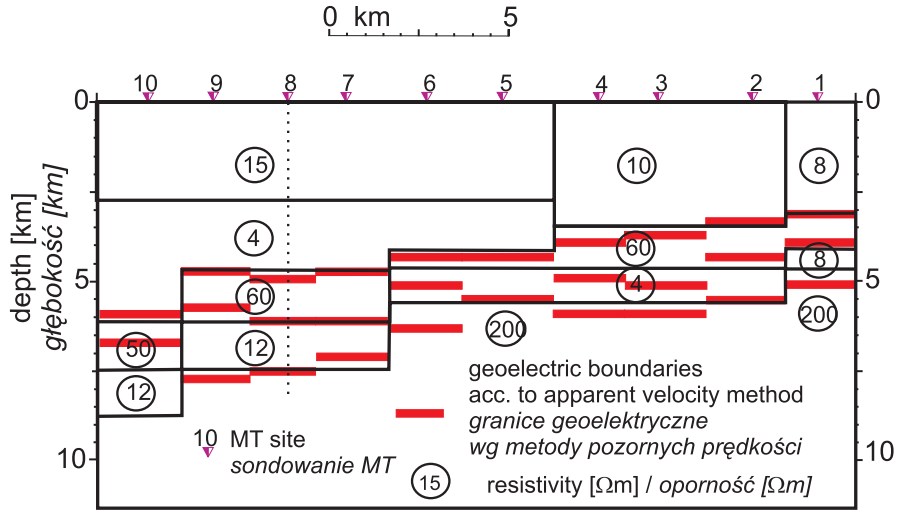
0 km 5
10 9 8 7 6 5 4 3 2 1
depth [km]
głębokość [km]
15
4
60
50
12
12
10
4
60
200
10
8
8
200
geoelectric boundaries
acc. to apparent velocity method
granice geoelektryczne
wg metody pozornych prędkości
10 MT site
sondowanie MT
15 resistivity [Ωm] / oporność [Ωm]

B)

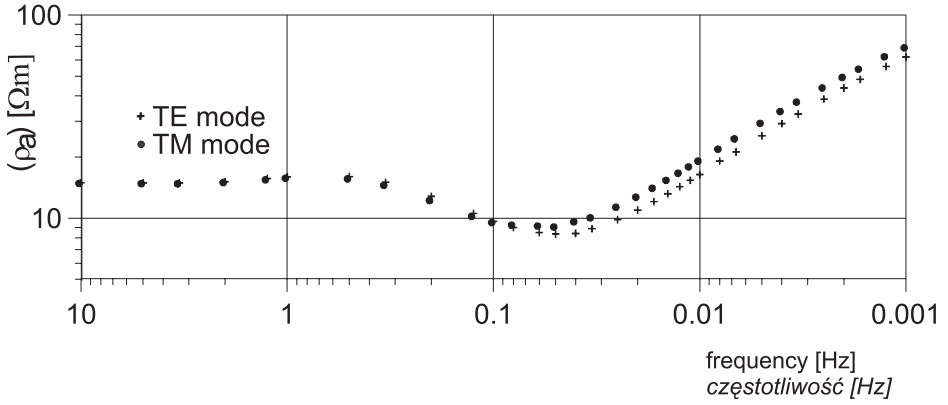
100
10
(ρa) [Ωm]
TE mode
TM mode
10 1 0.1 0.01 0.001
frequency [Hz]
częstotliwość [Hz]

C)

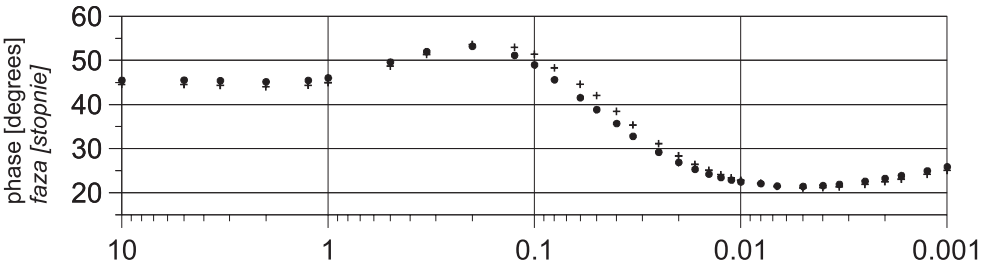
60
50
40
30
20
phase [degrees]
faza [stopnie]
10 1 0.1 0.01 0.001

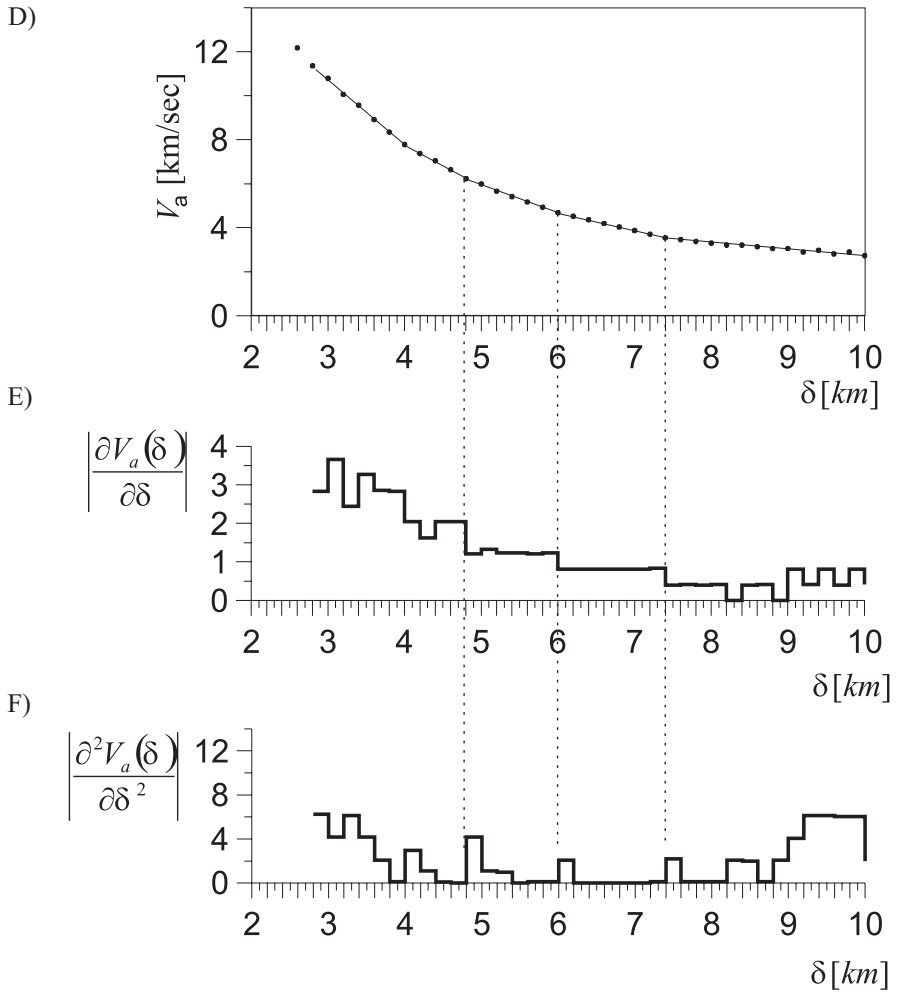


**Fig. 1.** Compilation of magnetotelluric curves (8 MT site) and geoelectric boundaries acc. to apparent velocity method for 2D synthetic model: A) 2D synthetic model with geoelectric boundaries acc. to apparent velocity method; B) $\rho_a$ – apparent resistivities for electric polarization (TE MODE++++) and magnetic polarization (TM MODE ••••); C) impedance phase; D) $V_a(\delta)$ – apparent velocity, δ – depth of penetration; E) derivative of $V_a(\delta)$ with geoelectric boundary acc. to apparent velocity method; F) second derivative of $V_a(\delta)$ with geoelectric boundaries acc. to apparent velocity method; ····· boundaries of layers

**Fig. 1.** Zestawienie krzywych sondowania MT (nr 8) oraz granic geoelektrycznych uzyskanych metodą pozornych prędkości dla modelu 2D: A) model 2D z granicami geoelektrycznymi uzyskanymi metodą pozornych prędkości: B) $\rho_a$ – oporność pozorna dla polaryzacji elektrycznej (TE MODE++++) i polaryzacji magnetycznej (TM MODE ••••); C) krzywe fazowe; D) $V_a(\delta)$ – prędkość pozorna, δ – głębokość; E) pierwsza pochodna $V_a(\delta)$ z zaznaczeniem granic geoelektrycznych uzyskanych metodą prędkości pozornej; F) druga pochodna $V_a(\delta)$ z zaznaczeniem granic geoelektrycznych uzyskanych metodą prędkości pozornej; ····· granice warstw

A)

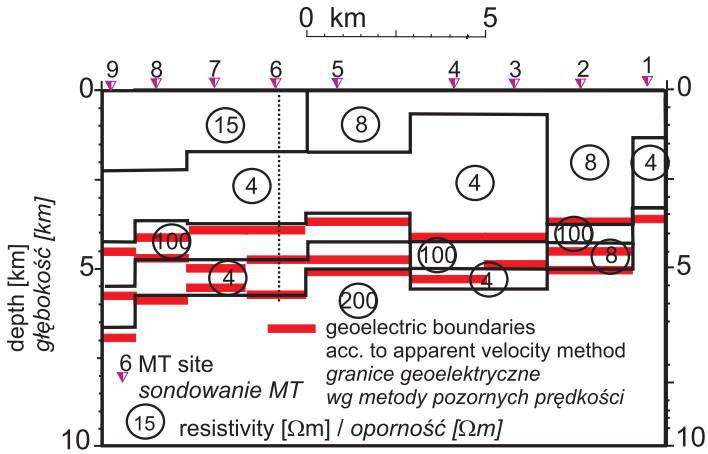
0 km
5
9
8
7
6
5
4
3
2
1
depth [km]
głębokość [km]
15
8
4
4
8
4
100
100
100
8
4
4
200
geoelectric boundaries
acc. to apparent velocity method
granice geoelektryczne
wg metody pozornych prędkości
6 MT site
sondowanie MT
15
resistivity [Ωm] / oporność [Ωm]

B)

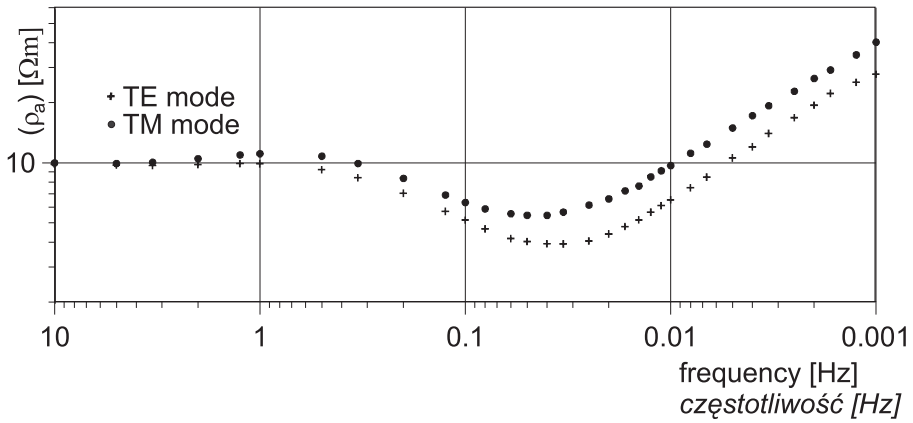
(ρa) [Ωm]
TE mode
TM mode
10
10
1
0.1
0.01
0.001
frequency [Hz]
częstotliwość [Hz]

C)

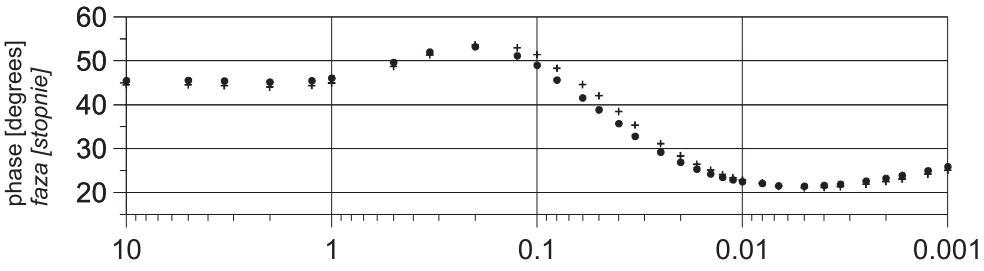
phase [degrees]
faza [stopnie]
60
50
40
30
20
10
1
0.1
0.01
0.001

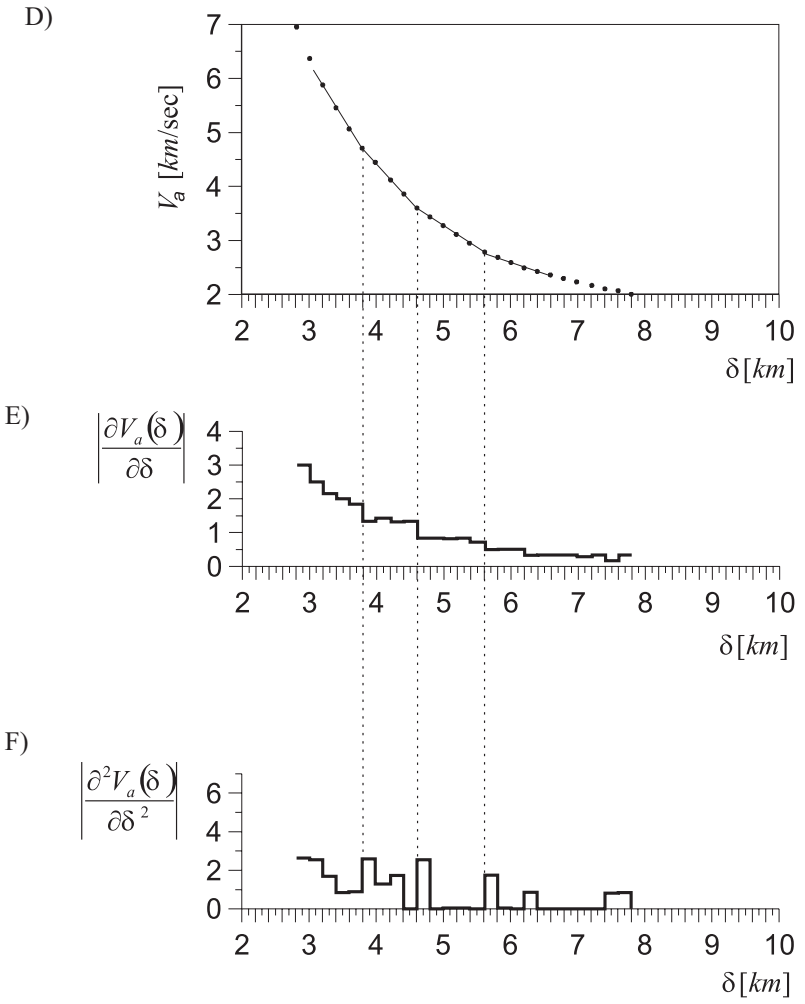


**Fig. 2.** Compilation of magnetotelluric curves (6 MT site) and geoelectric boundaries acc. to apparent velocity method for 2D synthetic model: A) 2D synthetic model with geoelectric boundaries acc. to apparent velocity method; B) $\rho_a$ – apparent resistivities for electric polarization (TE MODE ++++) and magnetic polarization (TM MODE ••••); C) impedance phase; D) $V_a(\delta)$ – apparent velocity, δ – depth of penetration; E) derivative of $V_a(\delta)$ with geoelectric boundary acc. to apparent velocity method; F) second derivative of $V_a(\delta)$ with geoelectric boundaries acc. to apparent velocity method; ····· boundaries of layers

**Fig. 2.** Zestawienie krzywych sondowania MT (nr 6) oraz granic geoelektrycznych uzyskanych metodą pozornych prędkości dla modelu 2D: A) model 2D z granicami geoelektrycznymi uzyskanymi metodą pozornych prędkości; B) $\rho_a$ – oporność pozorna dla polaryzacji elektrycznej (TE MODE ++++) i polaryzacji magnetycznej (TM MODE ••••); C) krzywe fazowe; D) $V_a(\delta)$ – prędkość pozorna, δ – głębokość; E) pierwsza pochodna $V_a(\delta)$ z zaznaczeniem granic geoelektrycznych uzyskanych metodą prędkości pozornej; F) druga pochodna $V_a(\delta)$ z zaznaczeniem granic geoelektrycznych uzyskanych metodą prędkości pozornej; ····· granice warstw

## EXAMPLE OF VISUALIZATION FROM THE EASTERN PART OF THE POLISH CARPATHIANS

The magnetotelluric survey was made by the PBG, Geophysical Exploration Company, Warsaw, Poland, in the eastern part of the Polish Carpathians. Ten magnetotelluric soundings were located along profile oriented perpendicularly to the strike (Fig. 3).

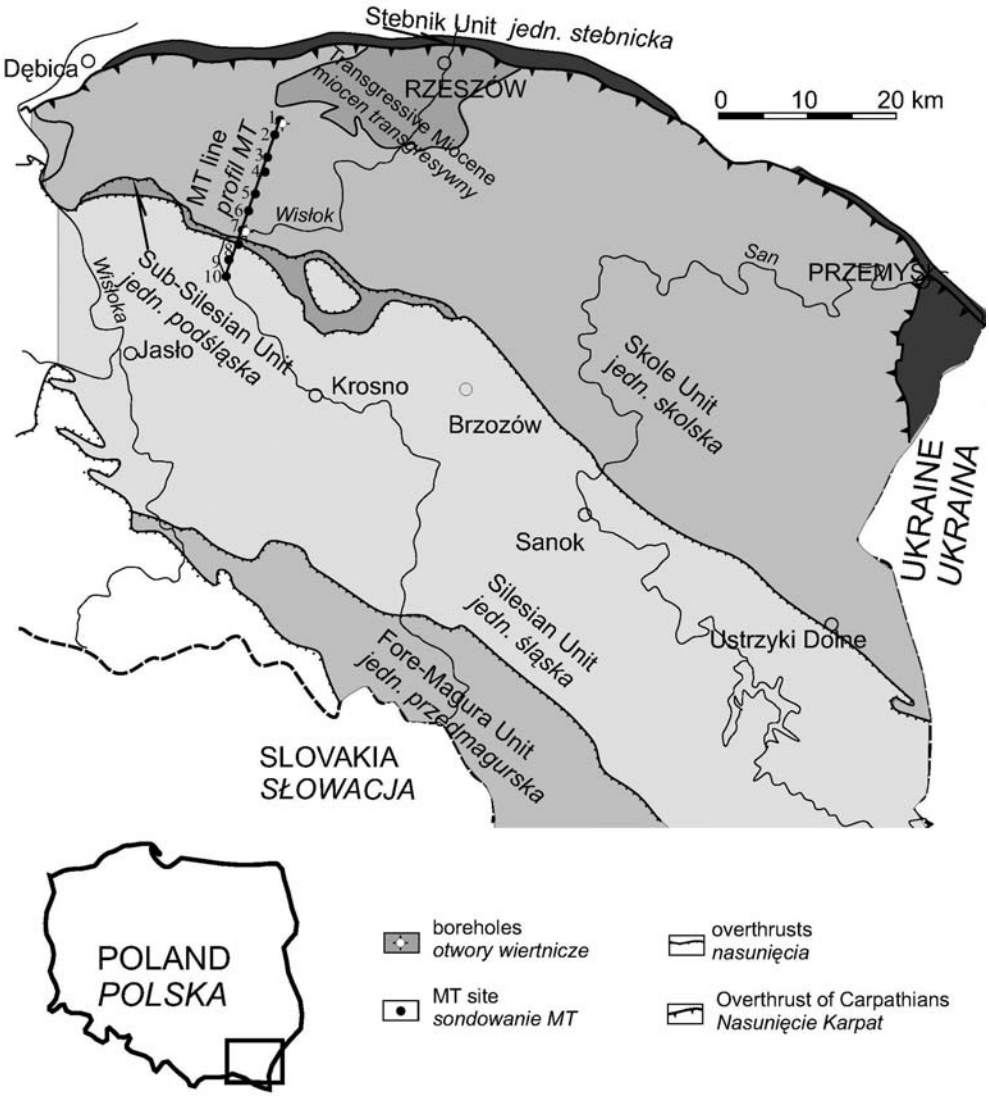


**Fig. 3.** Location of magnetotelluric profile from the Carpathian

**Fig. 3.** Lokalizacja profilu magnetotellurycznego w Karpatach

The goal of the project was the recognition of the structure of the roof of Mesopaleozoic, Lower Paleozoic and Precambrian basements. Integrated geophysical-and-geological interpretation with the use of seismic, well logging, gravity and magnetotelluric methods was made along the line shown in figure 3 (Stefaniuk *et al*. 2004). It delivers reliable information allowing for evaluation of apparent velocity method.

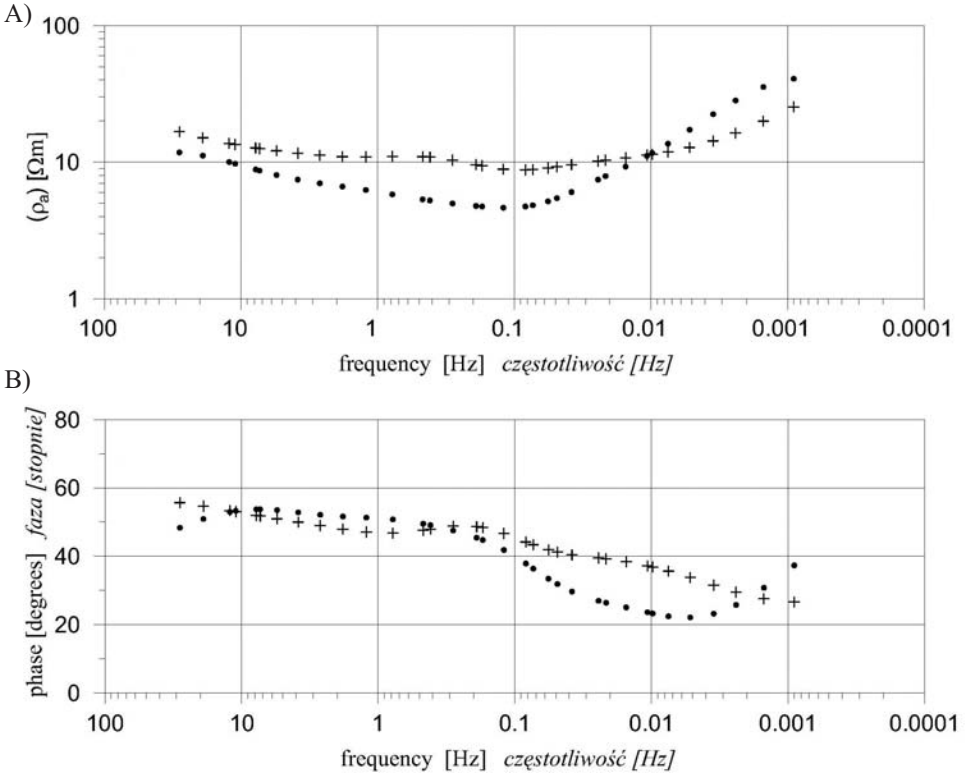


**Fig. 4.** Compilation of magnetotelluric curves (sounding no. 3, line – see Fig. 3): A) apparent resistivities for TE MODE (++++) and TM MODE (••••); B) impedance phases

**Fig. 4.** Krzywe sondowania magnetotellurycznego (nr 3, profil – patrz Fig. 3): A) oporność pozorna dla TE MODE (++++) oraz TM MODE (••••); B) krzywe fazowe

Figure 4 shows apparent resistivity and phase MT curves from selected magnetotelluric soundings (no. 3, Fig. 3). They are typical 2D curves from the Polish Carpathians (electric and magnetic polarization) where high-resistivity structures of Mesopaleozoic and Precambrian basement reflected at low frequencies. Low-resistivity structures (Stefaniuk *et al*. 2004) are characteristic for Lower Paleozoic.

Results of magnetotelluric data interpretation with the use of apparent velocity method are presented. Figure 5 shows distribution of apparent velocity ($V_a$) as a function of depth of penetration (δ) for this sounding (no. 3). It consists of straight line segments connected with geoelectric (thus geologic) layers and inclination of $V_a(\delta)$ change with resistivity com-

plexes. In that case first derivative of apparent velocity $\partial V_a(\delta)/\partial\delta$ changes at the boundary of geoelectric layers. Second derivative of apparent velocity $\partial^2 V_a(\delta)/\partial\delta^2$ curve on geoelectric boundary has big value (Fig. 5).

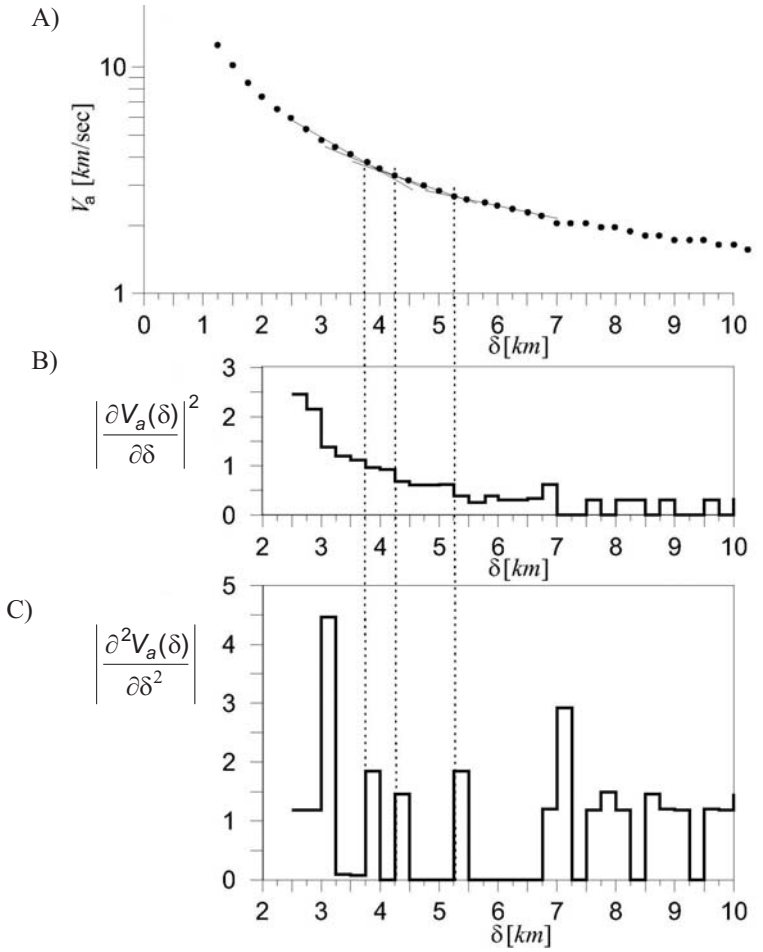


**Fig. 5.** Compilation of magnetotelluric curves (sounding no. 3, line – see Fig. 3): A) apparent velocity $V_a(\delta)$, $\delta$ – depth of penetration; B) derivative of $V_a(\delta)$; C) second derivative of $V_a(\delta)$

**Fig. 5.** Zestawienie krzywych sondowania MT (nr 3, profil – patrz Fig. 3): A) prędkość pozorna $V_a(\delta)$, $\delta$ – głębokość; B) pierwsza pochodna $V_a(\delta)$; C) druga pochodna $V_a(\delta)$

Results of numerical calculations for the discussed profile are shown in figures 6 and 7. Figure 6 shows apparent velocity cross-section along the line. The biggest change of apparent velocity at the upper part of geological section (in the flysh and Meso-Palezoic-Precambrian basements) is observed. Apparent velocity decreases with depth. Interpretation of geoelectric boundaries (thus geological) is not clear (Fig. 6).

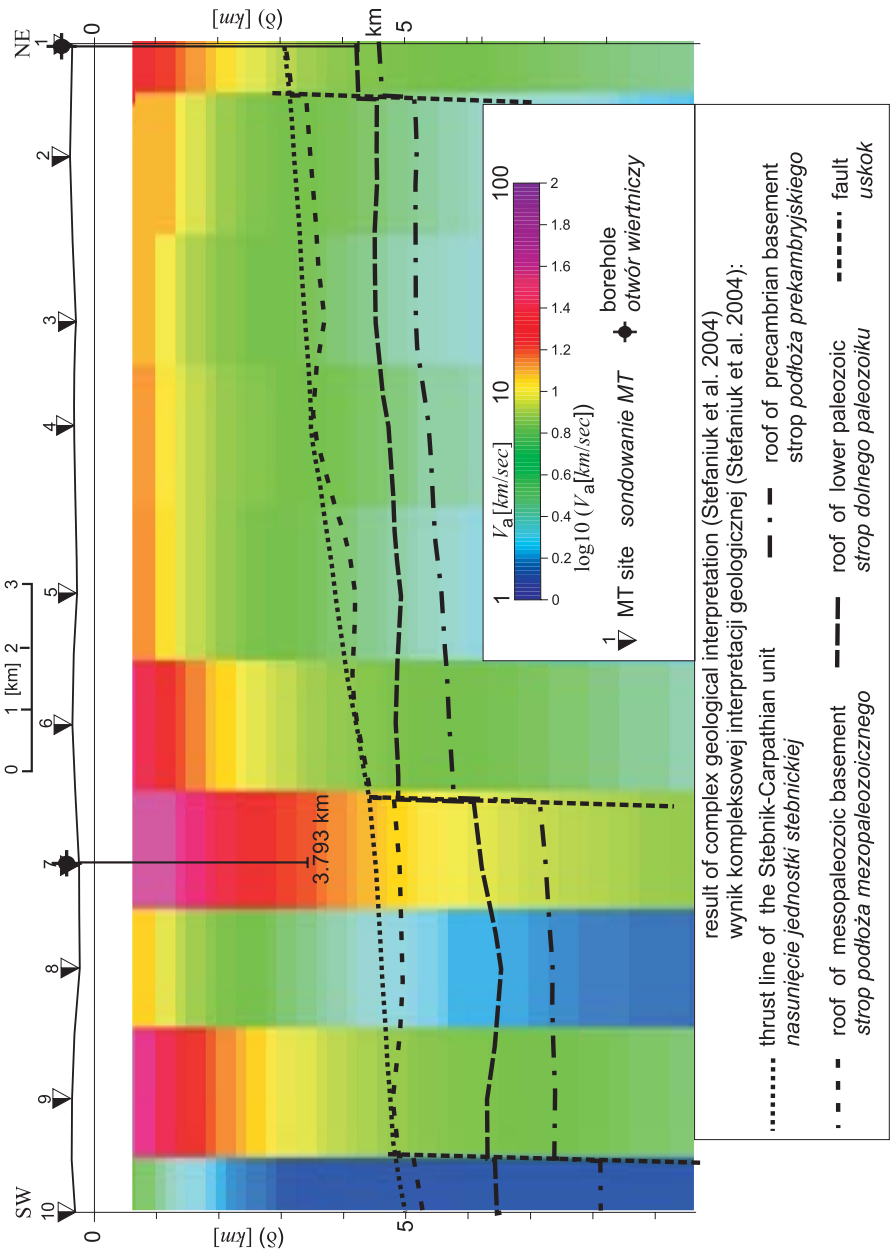


**Fig. 6.** 2D distribution of apparent velocity $V_a(\delta)$ [km/sec] (for line – Fig. 3)

**Fig. 6.** Rozkład 2D prędkości pozornej $V_a(\delta)$ [km/s] (dla profilu – patrz Fig. 3)

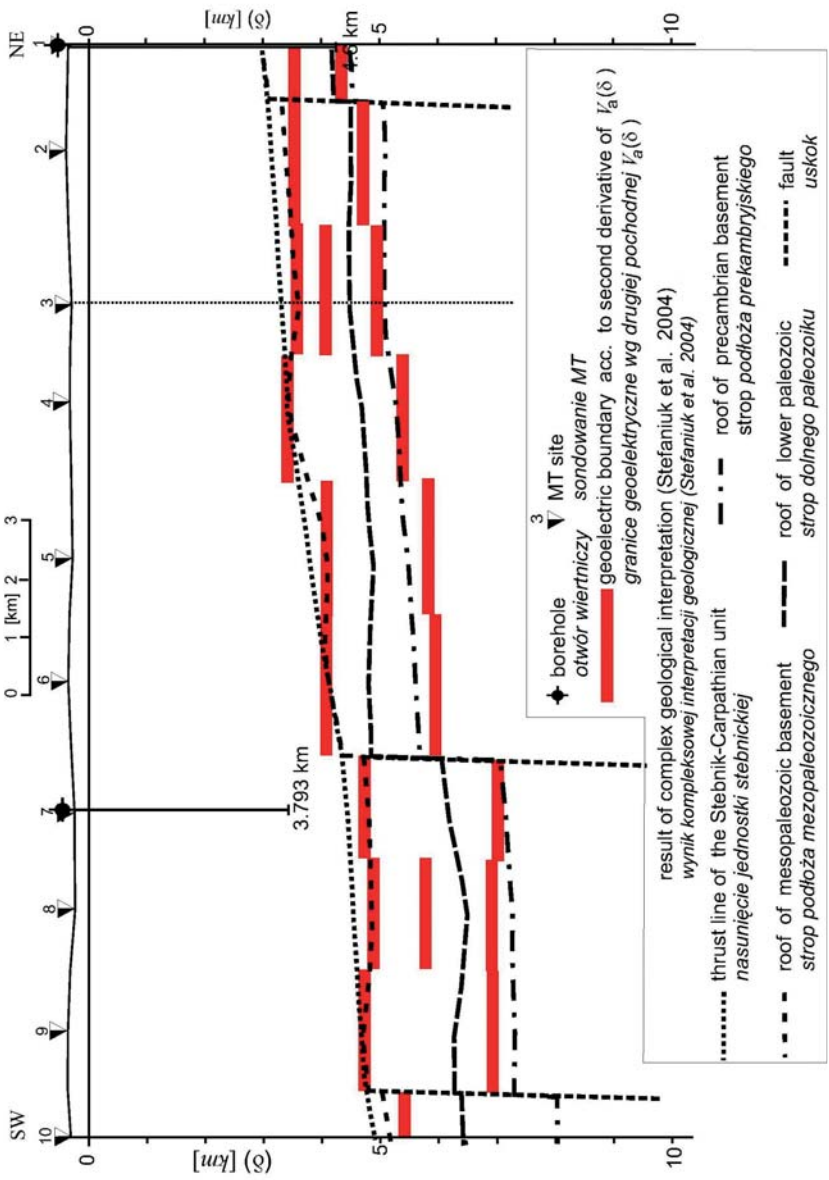


**Fig. 7.** Visualisation of magnetotelluric data using apparent velocity method (binary representation of second derivative of apparent velocity $\partial^2 V_a(\delta)/\partial\delta^2$, line – see Fig. 3)

**Fig. 7.** Wizualizacja danych magnetotellurycznych przy wykorzystaniu metody pozornych prędkości (reprezentacja binarna drugiej pochodnej prędkości pozornej $\partial^2 V_a(\delta)/\partial\delta^2$, profil – patrz Fig. 3)

Figure 7 shows distribution of the second derivative in the binary form. Extremely big values of the second derivative are presented as lines on the depth of penetration (with precision of step digitalization of $V_a(\delta)$ – here 250 meters, Fig. 5). They are connected with geoelectric boundaries and allow us to recognize Meso-Paleozoic and Precambrian basement.

They are well correlated with Meso-Paleozoic and Precambrian basement from geological cross-section. It is possible to determine the elevation of the Meso-Paleozoic basement close to MT site no. 4 (Fig. 7) using the apparent velocity method. This structure is important for recognition of hydrocarbons. The fault between soundings 6 and 7 and dip southward geological layers also occur. Possible geological lines in the flysch and in the Carpathian basement can be also observed (Fig. 7).

## SUMMARY

New possibilities for MT data interpretation are provided by using visualization of the apparent velocity method. A curve of apparent velocity $V_a$ versus depth of EM field penetration into the conducting earth ($\delta$) for each magnetotelluric sounding, can be approximated by straight-line segments corresponding to homogeneous geoelectric layer complexes. For this situation the first derivative of $V_a(\delta)$ on the geoelectric boundaries changes its value and the second derivative has relatively big value (that is manifested by incrementation). So, the first derivative and the second derivative of apparent velocity curve indicate geoelectric boundaries (Figs 1, 2). The obtained MT data interpretation from the Polish Carpathians (from the site close to borehole – Fig. 4, from the line where we have reliable information – Figs 5–7) point out that apparent velocity method can be used as an alternative and effective method to identify geoelectric (thus geologic) complexes.

## REFERENCES

Levv S., Oldenburg D. & Wang J., 1988. Subsurface imaging using magnetotelluric data. *Geophysics*, 53, 104–114.

Lee K.H., Liu G. & Morrison H.F., 1989. A new approach to modeling the electromagnetic response of conductive media. *Geophysics*, 54, 9, 1180–1192.

Lee K.H. & Xie G., 1993. Subsurface imaging using magnetotelluric data. *Geophysics*, 56, 6, 780–196.

Miecznik J. & Czerwiński T., 2001. Electromagnetic energy velocity in magnetotelluric sounding interpretation. *Abstracts of 63th EAGE Conference and Exhibition, Amsterdam*, 1–4, M-24.

Miecznik J., Gajewski A. & Czerwiński T., 2002.Electromagnetic Energy Velocity in Non--homogeneous media. A*bstracts of 64th EAGE Conference and Exhibition, Florence*, 1–4, D-14.

Molochnov G.W., 1968. Interpretacia magnitotelluriceskich zondirovanij s ispolzovaniem efektivnoj glubiny proniknovenia elektromagnitnogo pola. *Fizika Zemli*, 9, 88–94.

Stefaniuk M., Wojdyła M., Maksym A., Czerwiński T. & Klityński W., 2004. The structure of the Carpathians basement in the area between Jaslo and Rzeszow as a result of magnetotelluric data interpretation. W: *AAPG European region conference with GSA: regional geology and hydrocarbon systems of European & Russian Basins: looking for sweet spots: October 10–13, 2004 Prague, official program & abstract book, The Geological Society of America, Czech Geological Survey (Host Society), Tulsa, OK USA, AAPG Convention Department*, 109.

Wainstain L.A., 1963. *Fale elektromagnetyczne*. PWN, Warszawa, 257–302.

## Streszczenie

Metoda wizualizacji prędkości pozornej pozwala na rozszerzenie możliwości interpretacyjnych danych magnetotellurycznych. Krzywe prędkości pozornej $V_a$ w funkcji głębokości penetracji pola elektromagnetycznego w głąb przewodzącej ziemi (δ) dla każdego sondowania MT mogą być aproksymowane odcinkami prostymi. Każdy z tych odcinków prostych związany jest z jednorodnymi warstwami geoelektrycznymi. W tej sytuacji pierwsza pochodna prędkości pozornej $V_a(\delta)$ na granicach warstw geoelektrycznych zmienia wartość. Druga pochodna prędkości pozornej $V_a(\delta)$ ma na tych granicach relatywnie wysoką wartość (skokową). Jak widać, pierwsza i druga pochodna krzywych prędkości pozornej $V_a(\delta)$ wskazuje granice geoelektryczne (Fig. 1, 2). Uzyskane wyniki interpretacji metodą pozornych prędkości na przykładzie profilu z Karpat, w przypadku którego mamy wiarygodne informacje dotyczące budowy geologicznej (Fig. 5–7), wskazują na to, że wizualizacja pozorna prędkości może być efektywna i stanowić metodę alternatywną wobec identyfikacji geoelektrycznych (także geologicznych) kompleksów.